Experimental Cell Research 442 (2024) 114197

Contents lists available at ScienceDirect

Experimental Cell Research

journal homepage: www.elsevier.com/locate/yexcr

Research article

Integration of single-cell datasets depicts profiles of macrophages and fibro/adipogenic progenitors in dystrophic muscle

Alessandra Vitaliti [a,1], Alessio Reggio [b,1], Marta Colletti [c], Angela Galardi [c], Alessandro Palma [d,*]

[a] Department of Chemical Science and Technologies, "Tor Vergata" University of Rome, Viale della Ricerca Scientifica 1, 00133, Rome, Italy
[b] Department of Biology, University of Rome "Tor Vergata", Viale della Ricerca Scientifica 1, 00133, Rome, Italy
[c] Hematology/Oncology and Cell and Gene Therapy Unit, IRCCS, Ospedale Pediatrico Bambino Gesù, Piazza di Sant'Onofrio, 4, 00165, Rome, Italy
[d] Department of Biology and Biotechnologies "Charles Darwin", Sapienza University of Rome, Piazzale Aldo Moro 5, 00185, Rome, Italy

ARTICLE INFO

Keywords:
Muscle regeneration
Macrophages
Fibro/adipogenic progenitors
Single-cell
Genomics

ABSTRACT

Single-cell technologies have recently expanded the possibilities for researchers to gain, at an unprecedented resolution level, knowledge about tissue composition, cell complexity, and heterogeneity. Moreover, the integration of data coming from different technologies and sources also offers, for the first time, the possibility to draw a holistic portrait of how cells behave to sustain tissue physiology during the human lifespan and disease.

Here, we interrogated and integrated publicly available single-cell RNAseq data to advance the understanding of how macrophages, fibro/adipogenic progenitors, and other cell types establish gene regulatory networks and communicate with each other in the muscle tissue. We identified altered gene signatures and signaling pathways associated with the dystrophic condition, including an enhanced Spp1-Cd44 signaling in dystrophic macrophages. We shed light on the differences among dystrophic muscle aging, considering wild type, mdx, and more severe conditions as in the case of the mdx-2d model. Contextually, we provided details on existing communication relations between muscle niche cell populations, highlighting increased interactions and distinct signaling events that these cells stablish in the dystrophic microenvironment.

We believe our findings can help scientists to formulate and test new hypotheses by moving towards a more complete understanding of muscle regeneration and immune system biology.

1. Introduction

Muscle regeneration is a tightly regulated process involving the coordinated action of various cell types. These include immune system cells and mesenchymal cells, which collectively provide the muscle niche with essential environmental cues to facilitate proper regeneration [1–5].

Within the framework of inflammation, immune cells play a pivotal role by secreting both pro- and anti-inflammatory molecules that influence the muscle regeneration process [3]. Notably, macrophages are recognized as key orchestrators of this process. Initially, they polarize to a pro-inflammatory (M1-like) phenotype, creating an inflammatory environment at the site of muscle damage. Subsequently, they transition to an anti-inflammatory (M2-like) phenotype, promoting inflammation resolution during later stages of regeneration [2,5,6]. However, in dystrophic conditions characterized by persistent muscle fiber damage, M2-biased macrophages tend to assume a fibrogenic profile, exacerbating muscle damage and perpetuating inflammation [3,7,8].

This chronic inflammatory state alters the behavior of other niche members. In this regard, fibro/adipogenic progenitors (FAPs) persist in the site of damage and tend to adopt their mesenchymal fate by differentiating into adipocytes and fibroblasts [9,10]. Consequently, the deposition of these ectopic depots significantly complicates the clinical picture of muscular dystrophies [10–12]. In recent years, the tight relationship between immune cells and FAPs has emerged as a crucial regulator controlling FAP activation, proliferation, clearance, and differentiation [9,13]. However, these studies mainly stem from basic research approaches that marginally analyze binary cell relations by focusing on a single biological aspect. Therefore, overcoming such limitations by fully exploiting the content of multidimensional data may aid in deciphering in-depth all the molecular connections existing between immune cells and FAPs. The creation of an immune cell-FAP

* Corresponding author.
E-mail address: ale.palma@uniroma1.it (A. Palma).
[1] These authors contributed equally to this work.

https://doi.org/10.1016/j.yexcr.2024.114197
Received 17 May 2024; Received in revised form 2 August 2024; Accepted 3 August 2024
Available online 5 August 2024

interaction gene regulatory map will offer concrete druggable targets for optimizing and/or developing drug candidates meant to tackle the detrimental role of FAP cells in muscle diseases. To this end, we interrogated and integrated publicly available single-cell RNAseq data to unbiasedly extract multidimensional data from regenerating skeletal muscles at a single-cell resolution level. Hence, we identified altered gene signatures in the immune compartment and FAPs, and how such alterations impact the muscle niche.

2. Materials and methods

2.1. Single-cell RNA sequencing data processing

Publicly available scRNAseq dataset from WT, MDX and MDX 2D mouse muscles have been downloaded from the Gene Expression Omnibus (GEO) repository with accession IDs GSE213925 (wt, mdx, and mdx2D with NSG background), and GSE156498. Two additional WT scRNAseq samples were downloaded from Tabula Muris database (Skeletal muscle microfluidic emulsion https://figshare.com/articles/dataset/Single-cell_RNA-seq_data_from_microfluidic_emulsion_v2_/5968960). Single cell analysis has been performed using Seurat package in R environment (Version 5) [14]. We filtered out cells with less than 200 transcripts and followed a data processing pipeline using SCT transformation before the integration of the three datasets. We then run the computation of principal components (RunPCA function) and integrated the datasets using the HarmonyIntegration method. Next, we found neighbors using the first 30 principal components, clusters using a resolution = 0.01 and run the UMAP algorithm using the first 30 principal components and the harmony reduction. Markers were computed using the FindAllMarkers function, retrieving both positive and negative markers, with the following parameters: min.pct = 0.25, logfc.threshold = 0.25.

2.2. Cell populations annotation

Cell type identification has been performed using different approaches. After clustering analysis, we looked at the top expressed markers (ranked for decreasing log Fold Change) and identified genes that were expressed by distinct cell populations. To annotate clusters, we looked at the expression of the top gene markers on CellMarker 2.0 web server (http://bio-bigdata.hrbmu.edu.cn/CellMarker/index.html) with the "cell annotation" tool and selecting Mus Musculus species and "muscle" or "blood" (for immune system cells) tissues. We also checked for the expression of these markers on the Human Protein Atlas web server (https://www.proteinatlas.org/) in the single cell RNA expression tab, then selecting the "skeletal muscle" and "bone marrow" single cell tissues overview.

2.3. Pseudobulk analysis

For pseudobulk analysis, counts stored in the SCT slot of the Seurat object were used. Data has been aggregated by disease condition and sample using the AggregateExpression function of the Seurat package. Counts have been then extracted from the SCT slot. Normalization and differential expression testing has been then performed using DESeq2 package [15]. Statistical significance for differentially expressed genes was set based on the adjusted p-value <0.05 threshold. Enrichment analysis and plots of differentially expressed genes was performed using clusterProfiler R package [16] and Enrichr web tool (https://maayanlab.cloud/Enrichr/) [17]. Volcano plots have been drawn using EnhancedVolcano R package [18].

Spp1 analysis of macrophage has been performed by subsetting only the macrophage population. High and low Spp1 expression has been computed using the mean expression of Spp1 ± standard error mean (SEM) of Spp1. $Spp1^{high}$ macrophages are the cells whose expression of Spp1 is higher than the mean Spp1 value plus Spp1 SEM, whereas $Spp1^{low}$ cells are those with an Spp1 expression lower than the mean value of Spp1 minus Spp1 SEM.

2.4. Analysis of macrophage polarization

The single cell object has been subset to select only macrophage population. M1 and M2 scores have been computed using the AddModuleScore function provided within the Seurat package using gene markers manually curated from literature as follows:

M1 genes: *Stat1*, *Stat3*, *Nos2*, *Il1b*, *Tnfa*, *Il1r2*, *Cxcr2*, *Cd68*, *Cd86*, *Fcgr2*, *Fcgr3*.

M2 genes: *Chil3*, *Retnla*, *Arg1*, *Stat6*, *Pparg*, *Tgfb*, *Il10*, *Cd163*, *Cd206*, *Mrc1*, *Rock2*.

The density plots in Fig. 2 D have been made with custom ggplot scripts. The polarization status has been assigned based on the M1 and M2 score using the following formula:

If M1 Score > M2 Score, polarization = M1, else polarization = M2.

2.5. High dimensional WGCNA analysis

High dimensional weighted gene co-expression network analysis was used to identify gene co-expression networks of cells via unsupervised clustering. A consensus analysis between mdx and wt samples has been performed using the hdWGCNA package [19,20] in R environment according to the reference vignette of consensus analysis (https://smorabit.github.io/hdWGCNA/articles/consensus_wgcna.html), changing some specific parameters as follows. In the "MetacellsByGroups function we set k = 20, max_shared = 12, min_cells = 50, target_metacells = 200. Soft power thresholds: 10 and 9. Differential network analysis between mdx and wt conditions has been performed using the Differential module eigengene (DME) analysis pipeline (https://smorabit.github.io/hdWGCNA/articles/differential_MEs.html). Gene ontology enrichment for each module and plotting was performed using EnrichR package using the 2023 Gene Ontology annotation.

2.6. Cell-to-cell interactions analysis

Cell-to-cell interactions have been computed using the CellChat package in R environment [21]. We followed the "Inference and analysis of cell-cell communication using CellChat" vignette for the overall interaction analysis (https://htmlpreview.github.io/?https://github.com/jinworks/CellChat/blob/master/tutorial/CellChat-vignette.html), and the "Comparison analysis of multiple datasets using CellChat" vignette for differential interaction analysis between mdx and wt conditions (https://htmlpreview.github.io/?https://github.com/jinworks/CellChat/blob/master/tutorial/Comparison_analysis_of_multiple_datasets.html).

2.7. Cytokine ELISA array

$CD45^{+}$ cells were isolated from 45-day old WT and MDX mice, using a magnetic bead cell sorting system, as previously described [11,22]. Purified cells, were lysed in cold RIPA buffer and lysates processed for the ELISA array. Array ID: GSM-CAA-4000, tebu-bio.

3. Results

3.1. Functional alterations in dystrophic muscle cells composition

To gain insights into the role of distinct cell populations in the framework of Duchenne muscular dystrophy, we analyzed three publicly available single-cell RNA sequencing datasets of muscle tissues derived from wild-type (WT) and dystrophic mice, including the mdx (MDX) and the more sever 2D-mdx (MDX 2D) conditions (see Materials and Methods section and Supplementary Fig. 1). A first characterization of the resulting dataset using known biomarkers led to the identification

of several clusters that were grouped according to the expression of distinct markers (Supplementary Table 1) into nine distinct cell populations. These clusters are composed of cell identities belonging to the muscle niche, including those from the immune system compartment (Fig. 1A and B). Most of the identified cells were macrophages and FAPs, constituting more than half of the entire cell repertoire (Fig. 1C). In terms of abundance, they were immediately followed by myofibroblasts, endothelial cells, erythroblasts, and myogenic cells. Upon initial inspection, changes in cell abundances between in dystrophic conditions were observed (Fig. 1D upper panel). Particularly, a marked increase in the macrophages discern in an unbiased manner MDX from WT muscles, which a higher number of these cells in the MDX 2D condition, resulting as an apparent measure of the severity of the dystrophic condition. Such peculiar change in the abundance of these populations indicates that an intense remodeling activity occurs in this tissue as a consequence of the genetic damage. Such increase resulted much higher when comparing 4 weeks and 8 weeks old mice (Fig. 1D lower panel), which was accompanied by an increased number of other cell populations with aging, including fibro/adipogenic progenitor cells. Conversely, we observed a decrease in the myofibroblasts numerosity occurring with both aging and disease status (Fig. 1D lower panel).

3.2. Macrophage polarization status analysis

In the analyzed dataset, macrophages were the cell population showing the most dramatic changes in terms of cell abundance. To delineate the transcriptome of dystrophic macrophages and uncover their role in dystrophic settings, we evaluated their polarization state using a meticulously curated list of genes sourced from the literature (see Materials and Methods). Intriguingly, we noted that an increase in the absolute number of M1-like macrophages in dystrophic tissue, with markedly higher numbers in the MDX 2D condition (Fig. 2A). Using a gene scored based on well-known macrophage polarization gene markers, we noted that their transcriptional phenotype displayed heightened M1 and M2 scores, with a subpopulation of macrophage exhibiting a higher shift in both the M1 and M2 scores (Fig. 2B) in the MDX condition, and with an even higher shift to M1-like polarization state in the MDX 2D muscles. In contrast, WT macrophages exhibited a tendency towards being more unpolarized. It is worth to note that the conventional M1/M2 macrophage paradigm has been challenged by the notion that these cells often do not adhere strictly to well-defined polarized phenotypes but rather exist along a continuum of polarization states [5,23]. Therefore, we may speculate that dystrophic macrophages exhibit a hybrid phenotype, wherein we observe, at the transcriptional level, a blend of pro- and anti-inflammatory signatures. These signatures are given by the expression of both pro- and anti-inflammatory genes (see Materials and methods), in both WT and dystrophic conditions, including MDX and MDX 2D (Supplementary Fig. 2).

3.3. Pseudobulk analysis reveals Spp1 as a discriminant of dystrophic macrophages

Next, we focused our attention on macrophages implying that their increase may largely impact the dystrophic microenvironment. Specifically, we aimed at discerning potential disparities in the transcriptional

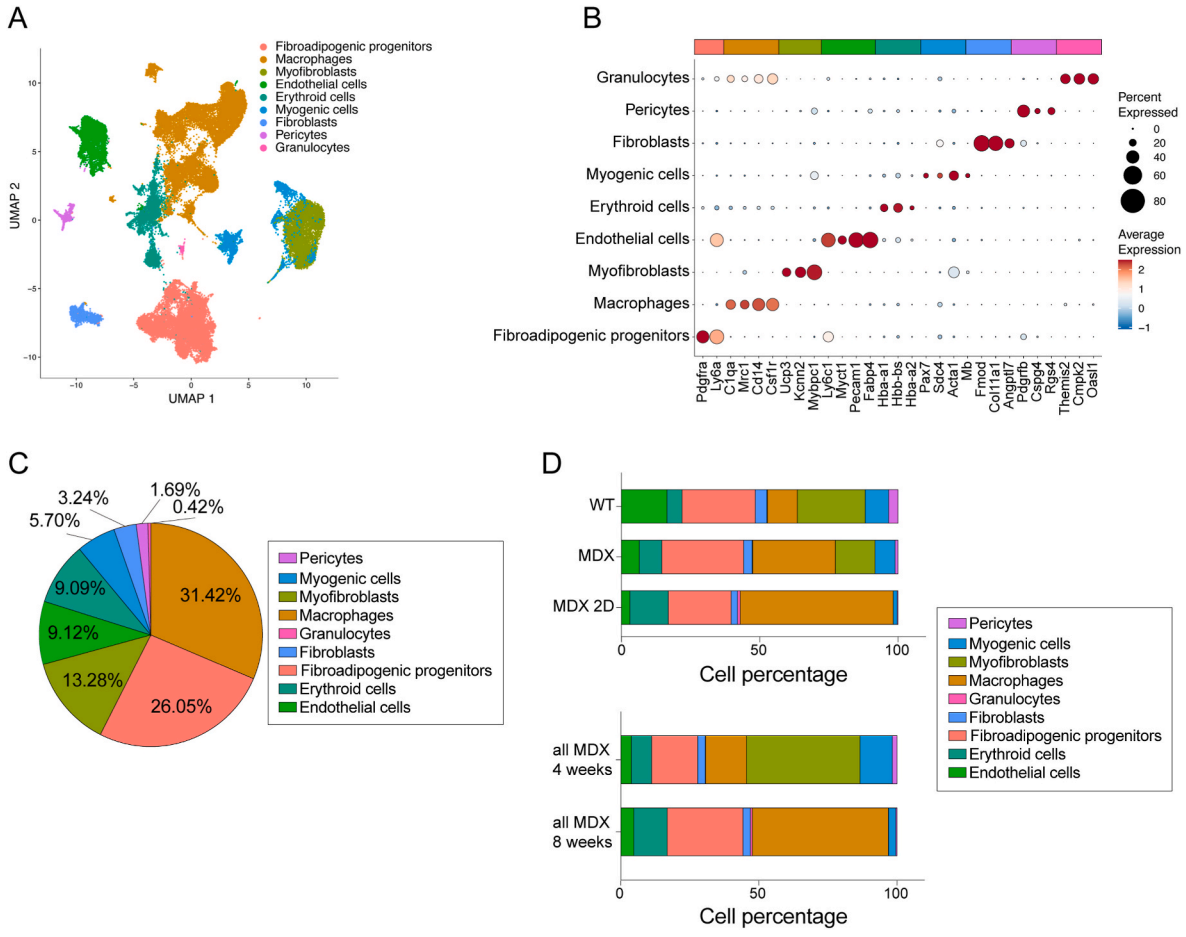

Fig. 1. Cell composition analysis of the muscle niche. (A) UMAP projection depicting the 9 distinct cell populations identified in the dataset. (B) Dotplot illustrating the expression of cell population-specific markers utilized for cell type annotation. (C) Pie chart presenting the percentage distribution of each cell population within the dataset. (D) Stacked barplot demonstrating the variations in cell abundances of WT, MDX, and MDX 2D muscles (upper panel), and in aging muscle (lower panel).

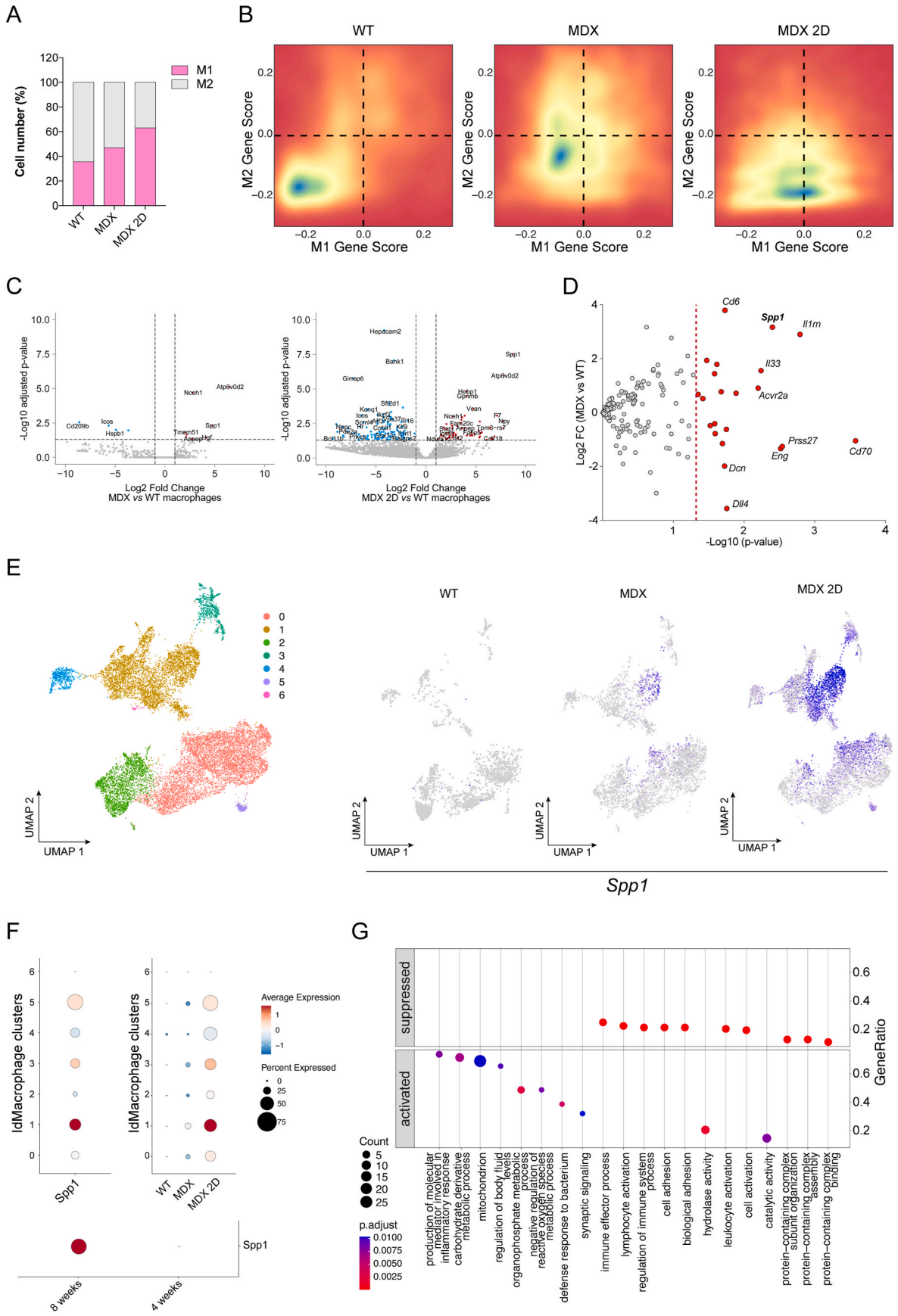

(caption on next page)

Fig. 2. Gene expression analysis of macrophages (A) Barplot showing the absolute number of macrophages classified as M1 or M2 in the WT, MDX, and MDX 2D samples. (B) Density plots depicting the M1-like and M2-like macrophage polarization scores. 8C) Volcanoplot reporting the differentially expressed genes in MDX vs WT (left panel) and MDX 2D vs WT (right panel). (D) Multiplex ELISA showing the significant (p-value >0.05) cytokines expressed by MDX macrophages compared to WT ones. (E) UMAPs reporting the macrophage subset (left panel) grouped by clusters and the expression of Spp1 gene (right panel) split by condition (WT, MDX, and MDX 2D). (F) Dot plots showing the expression of Spp1 gene in all macrophage clusters (left panel), in macrophage clusters split by condition (right panel), and in MDX macrophages by age (lower panel). (G) Gene set enrichment analysis of macrophage cluster 1, the cluster with the higher expression of Spp1 among macrophages.

profiles of this cell population between the dystrophic and WT conditions. To address this objective, we conducted a pseudobulk analysis by aggregating cells belonging to each cluster (cell population), grouped by samples, and performed a differential expression analysis. Numerous differentially expressed genes (DEGs) were identified across the majority of cell populations, with macrophages and FAPs exhibiting the highest number of DEGs (Supplementary Table 2). Focusing on macrophages, the osteopontin gene (Spp1) emerged as one of the most up-regulated genes in MDX muscles (Fig. 2C left panel), and even more in MDX 2D condition (Fig. 2C right panel). Notably, a distinct macrophage population expressing high levels of Spp1, often found as tumor-associated macrophages, has been previously characterized and linked to fibrotic outcomes in the heart [24]. Additionally, gene set enrichment analysis (GSEA) conducted on statistically significant genes (adj. p-value <0.05) unveiled that the most enriched process of Spp1 cluster is associated to the production of immunomodulatory mediators that are involved in inflammation.

From these premises, we focused our attention on Spp1 gene, subsetting our data and separately analyzed only the macrophage cluster. We were able to find 7 clusters (Fig. 2E), one of which (cluster 1) expressed high levels of Spp1, which was found to be up-regulated in dystrophic conditions, with the highest expression in the MDX 2D muscle (Fig. 2F), highlighting the possible role of this macrophage population dystrophic settings. Nevertheless, Spp1 was also the most up-regulated marker for this cluster compared to all the other clusters (Fig. 2G).

To go in depth into the analysis of the Spp1 macrophage population, we virtually binned it into two major groups on the basis of the expression level of Spp1 ($Spp1^{low}$ and $Spp1^{high}$). The differential expression testing between $Spp1^{high}$ and $Spp1^{low}$ macrophages resulted in 186 DEGs, which were almost all up-regulated (Supplementary Table 3). Enrichment analysis on these genes demonstrated a function for these sub-set of macrophages in inflammatory responses and in different metabolic processes (Fig. 2G), evidencing a possible role in establishing or maintaining an inflammatory environment. Consistently, $Spp1^{high}$ macrophages abundantly express profibrotic cytokines, including Il1a, Il1b, and Ccl4 (log2 fold change >2.3; Supplementary Table 3).

Based on these findings, we indicated $Spp1^{high}$ as the macrophage sub-population that may contribute to the establishment of an inflammatory and pro-fibrotic niche that irremediably impairs tissue function.

3.4. Analysis of FAPs transcriptional state

Since some of mediators coming from $Spp1^{hihg}$ and $Spp1^{low}$ macrophages are known to be modulators of FAP behavior, we focused our attention on FAP cells.

To this end, the differential expression analysis between MDX, MDX

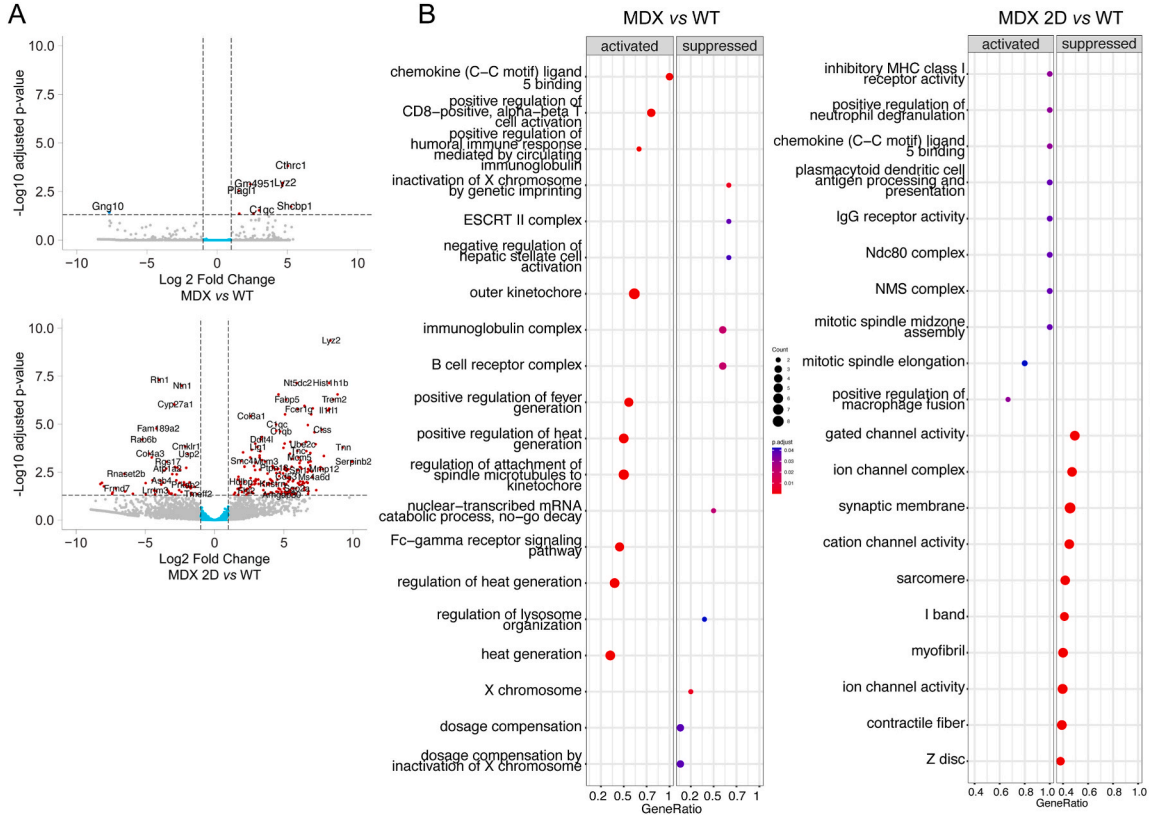

Fig. 3. Gene expression analysis of FAPs (A) Volcano plot showing the differentially expressed genes between MDX and WT (upper panel) and MDX 2D vs WT FAPs (lower panel). (B) GSEA plot illustrating the activated process resulting from the list of DEGs found in FAPs in the MDX vs WT (left panel) and MDX 2D vs WT (right panel) comparisons.

2D and WT FAPs revealed the upregulation of numerous genes involved in the phagocytosis of cellular debris, immune response, and cellular processes linked to membrane modeling (Fig. 3A and B), some of them previously reported by others [25]. Among the most upregulated genes in the MDX 2D, we identified lysozyme 2 (Lyz 2) (Fig. 3A), likely associated with the modulation of the sterile immune response in dystrophic muscle. Conversely, in the MDX-vs-WT comparison, we identified Cthrc1v (Fig. 3A), which has been reported as a prognostic marker for monitoring the severity of disease progression in Duchenne Muscular Dystrophy [26,27].

3.5. High dimensional WGCNA analysis dissects the regulatory networks in dystrophic muscles

To gain insights into the regulatory mechanisms underpinning the dystrophic condition, we leveraged high-dimensional Weighted Gene Co-expression Network Analysis (hdWGCNA). This type of analysis allowed us to look at gene regulatory networks, named "modules", established by distinct cell populations, and that could not be merely capture by looking at differential gene expression. Specifically, we conducted a consensus analysis to examine the presence of gene regulatory networks, or modules, that are conserved between dystrophic and WT conditions, and whether they are differentially regulated between the same conditions. Given that we observed the highest differences between the MDX 2D and WT muscle, we focused our attention on these two conditions.

Our analysis unveiled ten distinct modules (Fig. 4A), each representing different gene regulatory networks of co-expressed genes.

Interestingly, upon projecting these modules onto the single-cell dataset to assess their expression patterns, we observed enrichment in specific cell populations (Fig. 4B). Notably, the turquoise and pink modules exhibited pronounced expression in macrophages, while blue and black modules were enriched in FAPs. An in-depth analysis of these modules revealed that, although black and blue modules were upregulated in dystrophic FAPs (Fig. 4 C), they were not statistically significant.

Conversely, the turquoise and pink modules were notably enriched in macrophages. While the pink module exhibited upregulation in the dystrophic condition, demonstrating a statistically significant increase in processes associated with calcium-regulated activity, the turquoise

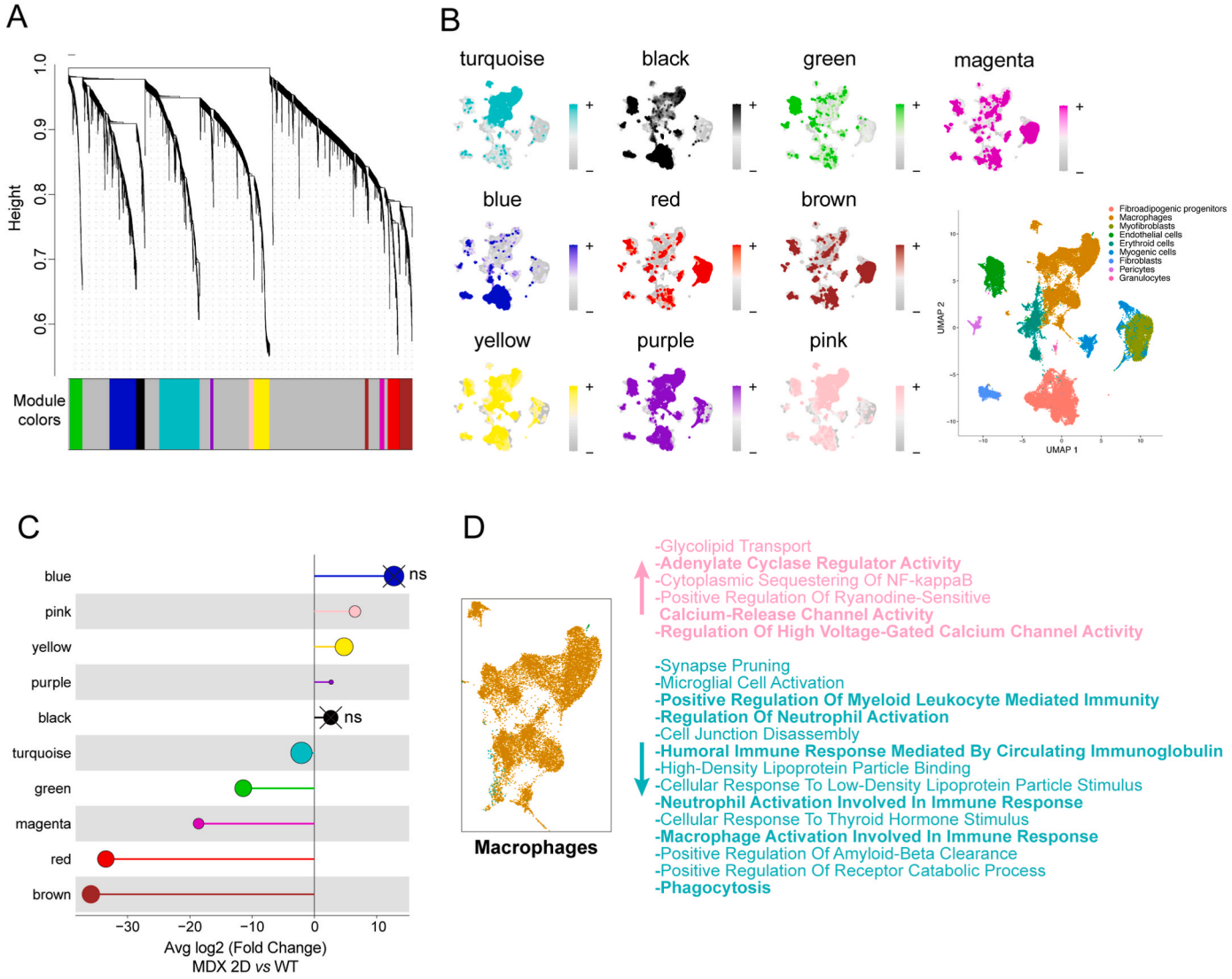

Fig. 4. Weighted gene correlation network analysis (A) Dendrogram illustrating the co-expression matrix, indicating the presence of ten distinct modules. (B) UMAP projections of kMEs displaying the expression of the modules across distinct clusters. (C) Lollipop plot depicting the log2 fold change of differentially expressed modules in the MDX 2D condition. Modules lacking statistical significance are denoted with an X. (D) Gene ontology (GO) enrichment analysis of genes belonging to specific modules. GO terms are color-coded according to the module name/color.

module was downregulated and enriched in GO terms linked to immune responses and macrophage activation (e.g. phagocytosis), corroborating the previous findings on the increased interactions and activity of dystrophic macrophages in the regulation of immune response functions.

These findings collectively suggest an participation role played by macrophages in dystrophic settings, with a dysregulation of their homeostasis linked to the establishment of chronic inflammation and the perpetuation of immune responses.

3.6. *Muscle-resident cells communicate with each other via specific signaling events*

Given the alterations in the transcriptional profiles of distinct cell populations in dystrophic muscle tissue, we explored whether such changes could impact cell-to-cell communication. To address this query, we analyzed interactions between cell populations predicted by the expression of ligand-receptor pairs, employing the CellChat package [28]. Upon considering the disparities between WT and MDX 2D conditions, we noticed a marked increase in terms of both number and strength of interactions in the MDX 2D condition (Fig. 5 A), which suggests that dystrophic muscles are characterized by intense signaling communications between cell populations. To go further into these interactions, we found that those involving FAPs, macrophages, granulocytes, and myofibroblasts appeared to be the most affected (Fig. 5 B). Specifically, we noted a notable increase in self-interactions among macrophages, alongside increased interactions from macrophages to myofibroblasts, granulocytes to macrophages, as well as FAPs to macrophages. In macrophages, the heightened outgoing interactions towards myofibroblasts and the self-interactions primarily revolved around the Spp1-Cd44 signaling axis (Fig. 5 C), reinforcing our previous findings regarding a potential pro-fibrotic role of this pathway within this cell population in dystrophic conditions.

When looking at differential incoming and outgoing interaction strength in MDX 2D muscle (Fig. 5D), we confirmed a significant increase in Spp1-Cd44 signaling, potentially indicating a response of these

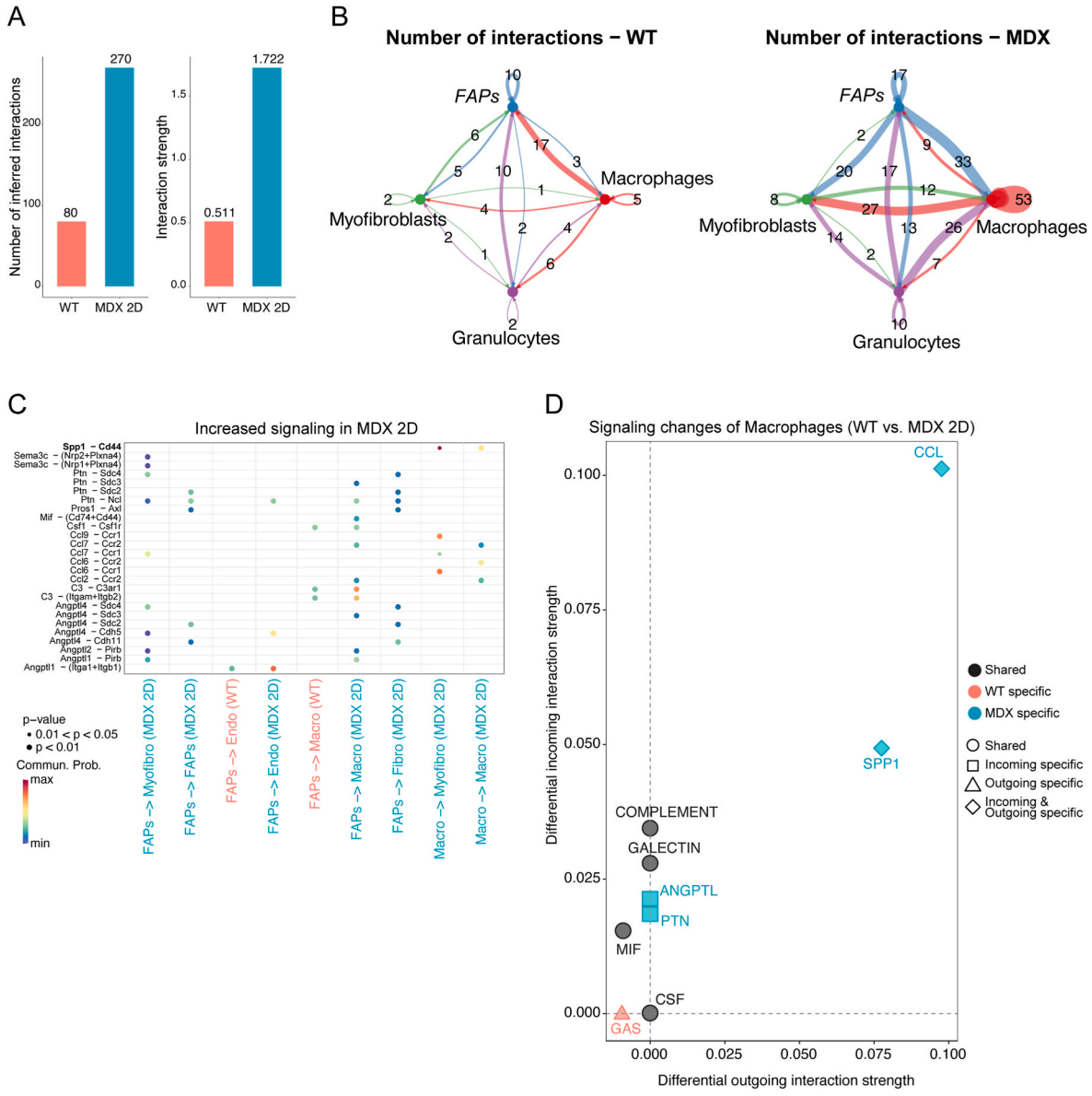

Fig. 5. Cell-to-cell interactions in the muscle niche (A) Barplot showing the differential number (left panel) and interaction strength (right panel) between the WT and MDX 2D conditions. (B) Interaction changes in terms of number between selected cell population in WT and MDX 2D muscles. (C) Heatmap showing specific signaling increases in FAPs and macrophages interactions in WT and MDX 2D conditions. (D) Scatterplot showing the signaling changes in macrophages in terms of both differential incoming and outgoing interaction strength.

cells to the fibrotic environment. Other important signaling events resulted increased in dystrophic conditions include the chemokine Ccl9 (also known as MIP-a alpha), in macrophage to myofibroblasts. This chemokine has been found up-regulated in dystrophic conditions [29] and it is known to be linked to the recruitment of macrophages and other immune cells within the dystrophic settings [30].

Collectively, these findings underscore an overall augmentation of cell-to-cell interactions in dystrophic conditions, highlighting a nuanced and dynamic interplay between immune and mesenchymal cells in establishing interactions that may be linked to aberrant processes and an attempt to resolve the inflammatory environment.

4. Discussion

The analysis of single-cell RNA sequencing datasets from wild-type and dystrophic mice muscle tissues, including the MDX and the more sever MDX 2D conditions, provided valuable insights into the role of distinct cell populations in muscular dystrophy. Our characterization identified nine distinct cell populations, with macrophages and FAPs comprising a substantial portion of the cellular repertoire. The observed changes in cell abundances suggest dynamic alterations within the dystrophic microenvironment, with macrophage representing a pivotal cell population particularly subject to changes in terms of cell abundance in dystrophic conditions.

In addition, we provided a picture of a possible hybrid polarization phenotype of dystrophic macrophages, which exhibit a heightened polarized transcriptional signature, with the MDX muscle showing an increased M1/M2 polarization, and the MDX 2D muscle characterized by macrophage with a M1-like polarized state. The existence of a macrophage population that is in an intermediate state between the canonical M1 and M2 phenotypes has been already discussed [4]. However, this nuanced understanding underscores the complexity of macrophage behavior in pathological states, highlighting the need for further investigation to elucidate the precise mechanisms underlying their functional plasticity. Additionally, biological processes enriched in MDX and MDX 2D macrophages highlighted their involvement in mitochondrial activity and inflammatory response, further emphasizing their contribution to the inflammatory milieu in dystrophic muscles. Indeed, the differential expression analysis revealed significant transcriptional differences between WT and MDX conditions, particularly in macrophages and FAPs. Dystrophic macrophages exhibited upregulation of pro-fibrotic markers like osteopontin (Spp1), indicating a shift towards a profile that resembles that observed in tumor-associated macrophages. Hence, we detailed how Spp1 marks a subset of profibrotic macrophages that likely influence other cell populations via soluble mediators, possibly imprinting in these cells a fibrogenic fate. This finding aligns with previous reports and underscores the role of macrophages in perpetuating inflammation and fibrosis in dystrophic muscles. Recently, a subset of FAPs expressing Spp1 was also reported and demonstrated capable to influence macrophage polarization [31]. In the present work, Spp1 was also expressed in FAPs but to a lesser extent than macrophages. These findings underscore a complex and underestimated role for Spp1 in autocrine signaling and cell-cell communication within the muscle niche.

When looking at FAPs transcriptional profile, the upregulation of genes associated with phagocytosis, immune response, and membrane modeling in mdx suggests their active involvement in dystrophic pathology. Notably, the identification of Cthrc1 among the upregulated genes highlights its potential as marker for disease severity in muscular dystrophies. Furthermore, the dysregulation of FAP-associated gene networks, particularly the upregulation of the red module enriched in endoplasmic reticulum vesicle transport, further implicates FAPs in matrix remodeling. Modules associated with FAPs also showed distinct regulatory patterns, indicating their pivotal role in orchestrating gene expression changes in response to dystrophic conditions.

Finally, the analysis of predicted ligand-receptor interactions revealed altered communication networks between cell populations in DMD muscles. Increased interactions, particularly involving macrophages, suggest heightened crosstalk between cells from the immune and other compartments in response to dystrophic cues. Notably, the upregulation of the Spp1-Cd44 signaling axis in macrophages and the complement signaling axis in FAPs-macrophages interactions may underlie the pro-fibrotic environment characteristic of dystrophic muscles.

Overall, our analysis of single-cell transcriptomics data sheds light on the intricate cellular dynamics underlying Duchenne Muscular Dystrophy. The observed alterations in cell populations, transcriptional profiles, and intercellular communication networks provide valuable insights into the pathogenesis of muscular dystrophy and highlight potential targets for mitigating disease progression. Further investigation into the functional implications of identified molecular signatures in FAPs and macrophages is needed to unravel the complex mechanisms driving dystrophic muscle pathology.

Funding

This research did not receive any specific grant from funding agencies in the public, commercial, or not-for-profit sectors.

CRediT authorship contribution statement

Alessandra Vitaliti: Writing – original draft, Visualization, Validation, Software, Resources, Methodology, Formal analysis, Data curation. **Alessio Reggio:** Writing – original draft, Visualization, Software, Resources, Methodology, Formal analysis, Data curation, Conceptualization. **Marta Colletti:** Visualization, Validation, Methodology, Formal analysis, Data curation. **Angela Galardi:** Visualization, Validation, Methodology, Formal analysis, Data curation. **Alessandro Palma:** Writing – review & editing, Visualization, Validation, Supervision, Software, Resources, Project administration, Methodology, Investigation, Formal analysis, Data curation, Conceptualization.

Declaration of competing interest

The authors declare that they have no known competing financial interests or personal relationships that could have appeared to influence the work reported in this paper.

Data availability

Data will be made available on request.

Acknowledgements

AP salary is provided by the European Union - NextGenerationEU: National Center for Gene Therapy and Drug based on RNA Technology, CN3 - Spoke 3 (code: CN00000041; PNRR MUR – M4C2 – Action 1.4-Call “Potenziamento strutture di ricerca e di campioni nazionali di R&S”, CUP: B83C22002870006). AR was supported by AFM-Téléthon grant number 23551.

Appendix A. Supplementary data

Supplementary data to this article can be found online at https://doi.org/10.1016/j.yexcr.2024.114197.

References

[1] A. Musarò, The basis of muscle regeneration, Adv. Biol. (2014) 1–16, 2014.
[2] J.G. Tidball, Regulation of muscle growth and regeneration by the immune system, Nat. Rev. Immunol. 17 (2017) 165–178.
[3] D.R. Lemos, et al., Nilotinib reduces muscle fibrosis in chronic muscle injury by promoting TNF-mediated apoptosis of fibro/adipogenic progenitors, Nat. Med. 21 (2015) 786–794.

[4] G. Juban, et al., AMPK activation regulates LTBP4-dependent TGF-β1 secretion by pro-inflammatory macrophages and controls fibrosis in Duchenne muscular dystrophy, Cell Rep. 25 (2018) 2163–2176.e6.
[5] L. Arnold, et al., Inflammatory monocytes recruited after skeletal muscle injury switch into antiinflammatory macrophages to support myogenesis, J. Exp. Med. 204 (2007) 1057–1069.
[6] R. Mounier, et al., AMPKα1 regulates macrophage skewing at the time of resolution of inflammation during skeletal muscle regeneration, Cell Metabol. 18 (2013) 251–264.
[7] M. Theret, M. Saclier, G. Messina, F.M.V. Rossi, Macrophages in skeletal muscle dystrophies, an entangled partner, J. Neuromuscul. Dis. 9 (2022) 1–23.
[8] M. Wehling-Henricks, et al., Arginine metabolism by macrophages promotes cardiac and muscle fibrosis in mdx muscular dystrophy, PLoS One 5 (2010).
[9] G. Giuliani, M. Rosina, A. Reggio, Signaling pathways regulating the fate of fibro/adipogenic progenitors (FAPs) in skeletal muscle regeneration and disease, FEBS J. 1 (2021) 16080 febs.
[10] A. Reggio, et al., Adipogenesis of skeletal muscle fibro/adipogenic progenitors is affected by the WNT5a/GSK3/β-catenin axis, Cell Death Differ. 27 (2020) 2921–2941.
[11] A. Reggio, et al., Metabolic reprogramming of fibro/adipogenic progenitors facilitates muscle regeneration, SSRN Electron. J. (2019), https://doi.org/10.2139/ssrn.3411252.
[12] A. Uezumi, et al., Fibrosis and adipogenesis originate from a common mesenchymal progenitor in skeletal muscle, J. Cell Sci. 124 (2011) 3654–3664.
[13] M. Theret, F.M.V. Rossi, O. Contreras, Evolving roles of muscle-resident fibro-adipogenic progenitors in health, regeneration, neuromuscular disorders, and aging, Front. Physiol. 12 (2021) 1–23.
[14] Y. Hao, et al., Dictionary learning for integrative, multimodal and scalable single-cell analysis, Nat. Biotechnol. 42 (2024) 293–304.
[15] M.I. Love, W. Huber, S. Anders, Moderated estimation of fold change and dispersion for RNA-seq data with DESeq2, Genome Biol. 15 (2014) 550.
[16] T. Wu, et al., clusterProfiler 4.0: a universal enrichment tool for interpreting omics data, Innovation 2 (2021) 100141.
[17] M.V. Kuleshov, et al., Enrichr: a comprehensive gene set enrichment analysis web server 2016 update, Nucleic Acids Res. 44 (2016) W90.
[18] K. Blighe, et al., EnhancedVolcano: Publication-Ready Volcano Plots with Enhanced Colouring and Labeling, 2024.
[19] S. Morabito, F. Reese, N. Rahimzadeh, E. Miyoshi, V. Swarup, hdWGCNA identifies co-expression networks in high-dimensional transcriptomics data, Cell Reports Methods 3 (2023).
[20] S. Morabito, et al., Single-nucleus chromatin accessibility and transcriptomic characterization of Alzheimer's disease, Nat. Genet. 53 (2021) 1143–1155.
[21] S. Jin, M.V. Plikus, Q. Nie, CellChat for systematic analysis of cell-cell communication from single-cell and spatially resolved transcriptomics, bioRxiv 11.05 (2023) 565674, 2023.
[22] A. Reggio, et al., The immunosuppressant drug azathioprine restrains adipogenesis of muscle Fibro/Adipogenic Progenitors from dystrophic mice by affecting AKT signaling, Sci. Rep. 9 (2019) 1–23.
[23] A. Sica, A. Mantovani, Macrophage plasticity and polarization: in vivo veritas, J. Clin. Invest. 122 (2012) 787–795.
[24] K. Hoeft, et al., Platelet-instructed SPP1+ macrophages drive myofibroblast activation in fibrosis in a CXCL4-dependent manner, Cell Rep. 42 (2023) 112131.
[25] J.E. Heredia, et al., Type 2 innate signals stimulate fibro/adipogenic progenitors to facilitate muscle regeneration, Cell 153 (2013) 376–388.
[26] Y.J. Liu, J. Du, J. Li, X.P. Tan, Q. Zhang, CTHRC1, a novel gene with multiple functions in physiology, disease and solid tumors (Review), Oncol. Lett. 25 (2023) 1–9.
[27] I. Spector, et al., The involvement of collagen triple helix repeat containing 1 in muscular dystrophies, Am. J. Pathol. 182 (2013) 905–916.
[28] S. Jin, et al., Inference and analysis of cell-cell communication using CellChat, Nat. Commun. 12 (2021).
[29] B. De Paepe, J.L. De Bleecker, Cytokines and chemokines as regulators of skeletal muscle inflammation: presenting the case of Duchenne muscular dystrophy, Mediat. Inflamm. 2013 (2013).
[30] J.D. Porter, et al., Persistent over-expression of specific CC class chemokines correlates with macrophage and T-cell recruitment in mdx skeletal muscle, Neuromuscul. Disord. 13 (2003) 223–235.
[31] X. Zhang, et al., Senescent skeletal muscle fibroadipogenic progenitors recruit and promote M2 polarization of macrophages, Aging Cell 23 (2024) 1–10.